The Record-Breaking Heat Wave in 2016 over South Korea and Its Physical Mechanism

SANG-WOOK YEH,[a] YOU-JIN WON,[a,b] JIN-SIL HONG,[a] KANG-JIN LEE,[c] MINHO KWON,[c] KYONG-HWAN SEO,[d] AND YOO-GEUN HAM[e]

[a] *Department of Marine Sciences and Convergence Technology, Hanyang University, Ansan, South Korea*
[b] *Korea Meteorological Administration, Seoul, South Korea*
[c] *KIOST, Busan, South Korea*
[d] *Pusan National University, Busan, South Korea*
[e] *Department of Oceanography, Chonnam National University, Gwangju, South Korea*

(Manuscript received 26 July 2017, in final form 1 March 2018)

ABSTRACT

It is important to understand the dynamical processes that cause heat waves at regional scales. This study examined the physical mechanism that was responsible for a heat wave in South Korea in August 2016. Unlike previous August heat waves over the Korean Peninsula, the intensity of the geopotential height over the Kamchatka Peninsula in August 2016 was the strongest since 1979, which acted as an atmospheric blocking in the downstream region of the Korean Peninsula. Therefore, the anomalous high geopotential height in Mongolia, where the surface temperature was quite high, was observed persistently in August 2016. This anomalous high in Mongolia induced northerly winds with warm temperatures onto the Korean Peninsula, which contributed to a heat wave in August 2016. We further showed that the anomalous high geopotential height over the Kamchatka Peninsula in August 2016 was triggered by strong convection in the western-to-central subtropical Pacific through atmospheric teleconnections, which was quite different from a typical heat wave over the Korean Peninsula, in which convective forcing around the South China Sea is strong. This implies that convective forcing in the subtropical Pacific should also be monitored to predict heat wave events in East Asia, including South Korea. On the other hand, the zonal wave train associated with the circumglobal teleconnection pattern is also associated with the anomalous high geopotential height around Mongolia and the Kamchatka Peninsula, which may have contributed to the heat wave in August 2016.

1. Introduction

A significant increase in greenhouse gas concentrations leads to a rapid increase in the surface air temperature on Earth (IPCC 2013). Along with the increase in mean surface temperature, extreme weather events such as heat waves, floods, and possibly intense typhoons have occurred more frequently in the past decades (Meehl and Tebaldi 2000; Coumou and Rahmstorf 2012; IPCC 2013). In particular, more attention has been paid to the characteristics of heat waves in recent years because the occurrence of heat waves directly affects crop productivity, power supplies, and water resource management, and it can also cause severe damage to both societies and economies (Karl and Quayle 1981; Kysely and Kim 2009; Kim et al. 2010; Coumou and Robinson 2013; Lee et al. 2016). According to the World Meteorological Organization (WMO 2013), the number of deaths due to heat waves for 2001–10 increased markedly by 2300%, compared to the number for 1991–2000. However, recent observations have shown that there exists a large diversity in the nature of heat waves from region to region (Cerne et al. 2007; Galarneau et al. 2012; García-Herrera et al. 2010; Jones et al. 2012; Coumou et al. 2014; Min et al. 2014; Coumou et al. 2015; Di Capua and Coumou 2016; Grotjahn et al. 2016; Yeo et al. 2017, 2018). This complexity requires a more comprehensive understanding of the dynamical processes leading to heat waves at regional scales. Therefore, it is important to understand the dynamical processes that cause regional heat waves. This study examines the physical mechanism that led to the August 2016 extraordinary heat wave in South Korea.

In August 2016, a strong, long-lasting heat wave with very high surface temperatures was observed in South Korea and some regions in East Asia (KMA 2016). The duration of the heat wave was 16.7 days, which broke the

Corresponding author: Prof. Sang-Wook Yeh, swyeh@hanyang.ac.kr

DOI: 10.1175/MWR-D-17-0205.1

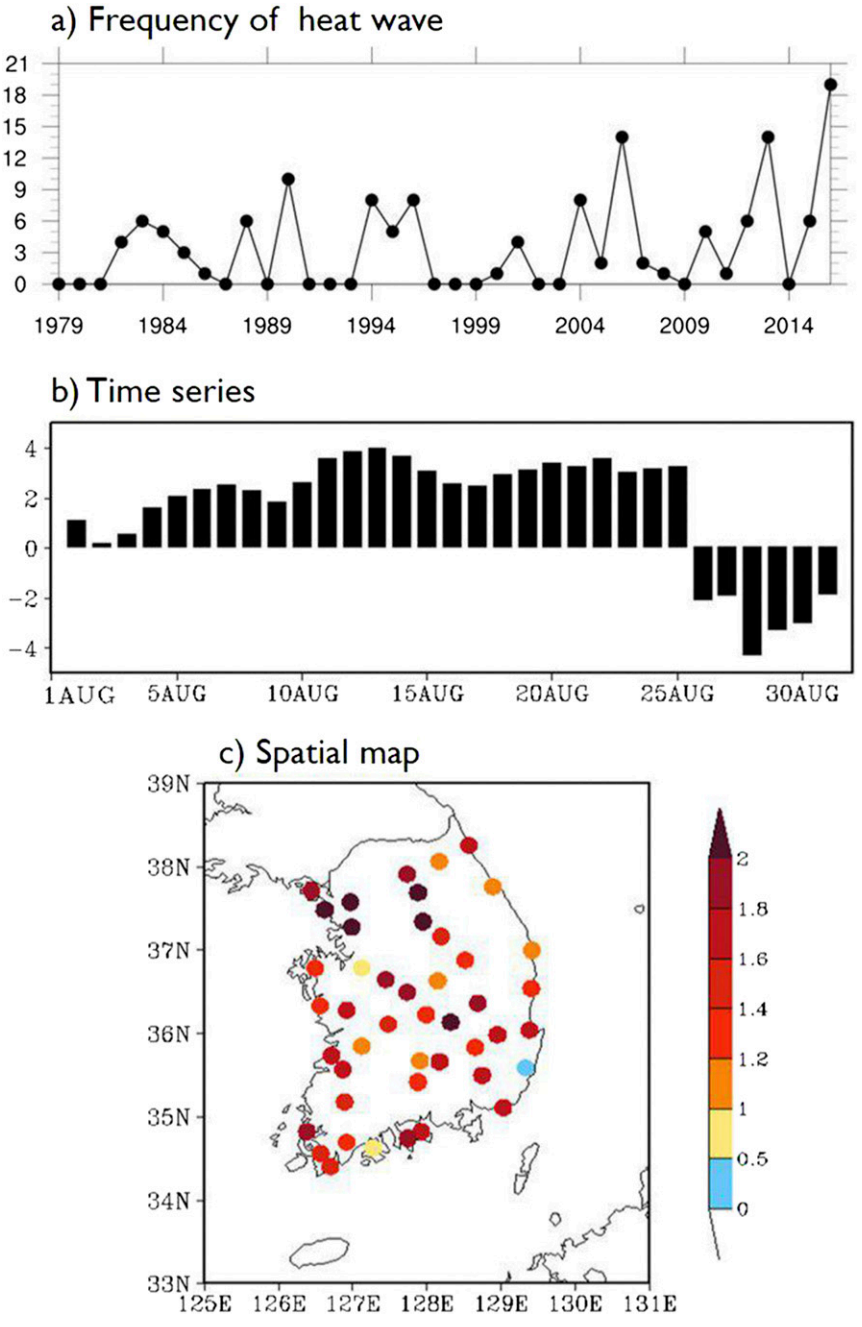

FIG. 1. (a) Time series of Korean heat wave frequency in August from 1979 to 2016. (b) Time series of daily Korean surface temperature anomalies in August 2016. (c) Spatial map of surface temperature anomalies observed at 45 weather stations in South Korea in August 2016. The climatological period is 1981–2010.

record set in 1973 (KMA 2016). Note that the Korea Meteorological Administration defines a heat wave as a period of at least 2 consecutive days where daily maximum temperature exceeds 33°C. Figure 1a displays the time series of heat wave frequency defined as the number of days when the daily maximum temperature is above the 90th percentile (i.e., 33.05°C) at the 45 weather stations in South Korea. The base period used in the definition of the 90th percentile is for the climatological period of 1981–2010. The frequency of heat wave number has been gradually increasing in South Korea since 1979, and it is the highest in 2016. In

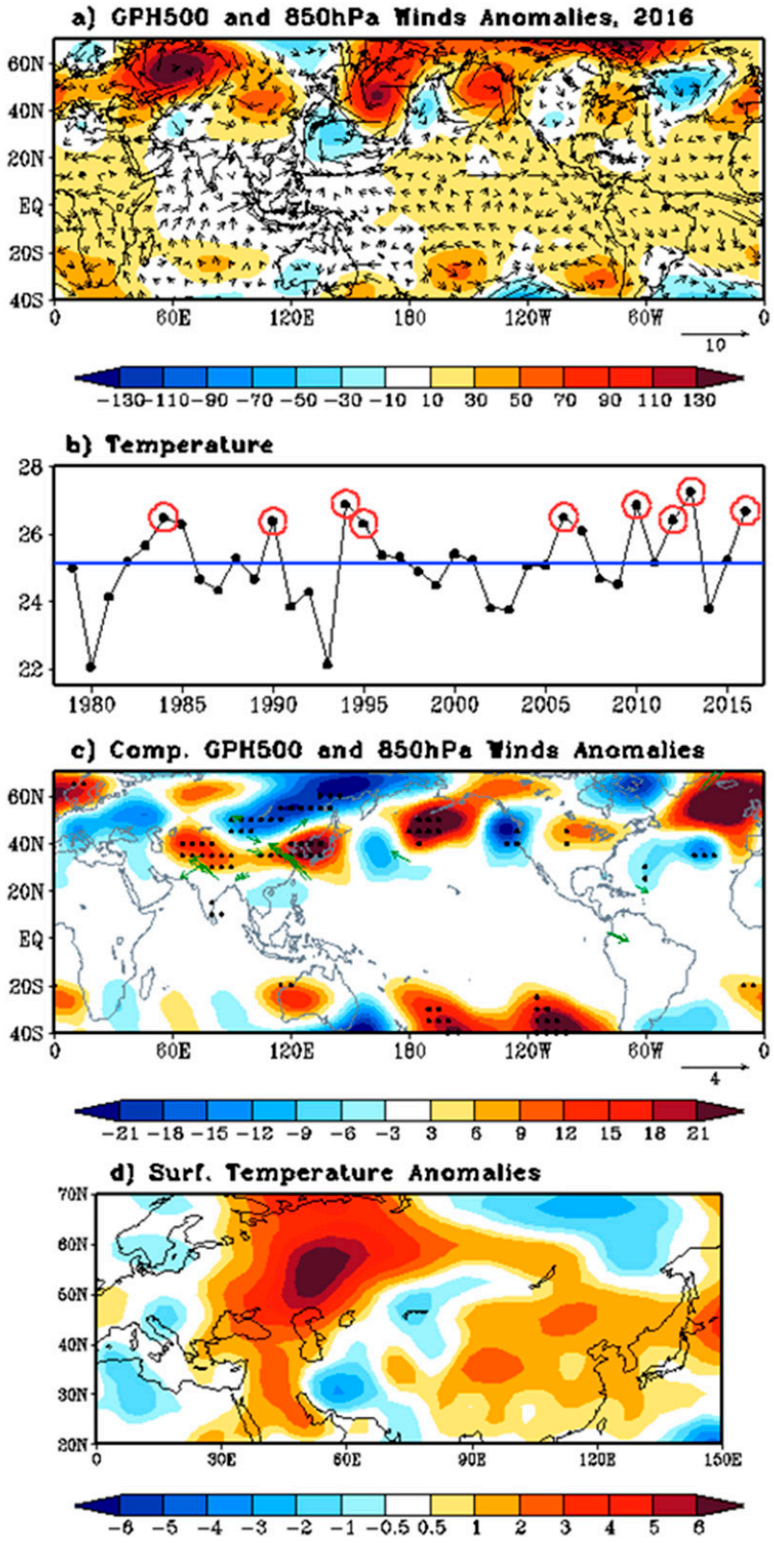

FIG. 2. (a) Anomalies of geopotential height at 500 hPa (shading; m) and winds at 850 hPa (vector; m s^{-1}) in August 2016. (b) Time series of Korean surface temperature (°C) in August for 1979–2016. Solid straight line indicates the climatological (1981–2010) mean surface temperature. (c) Composite of anomalous geopotential height at 500 hPa (shading; m) and winds at 850 hPa (vector; m s^{-1}) in 8 years [1984, 1990, 1994, 1995, 2006, 2010, 2012, and 2013; open circle in (b)]. (d) As in (a), but for surface temperature (°C). Dots and wind vectors in (c) denote the statistical significance at the 95% confidence level.

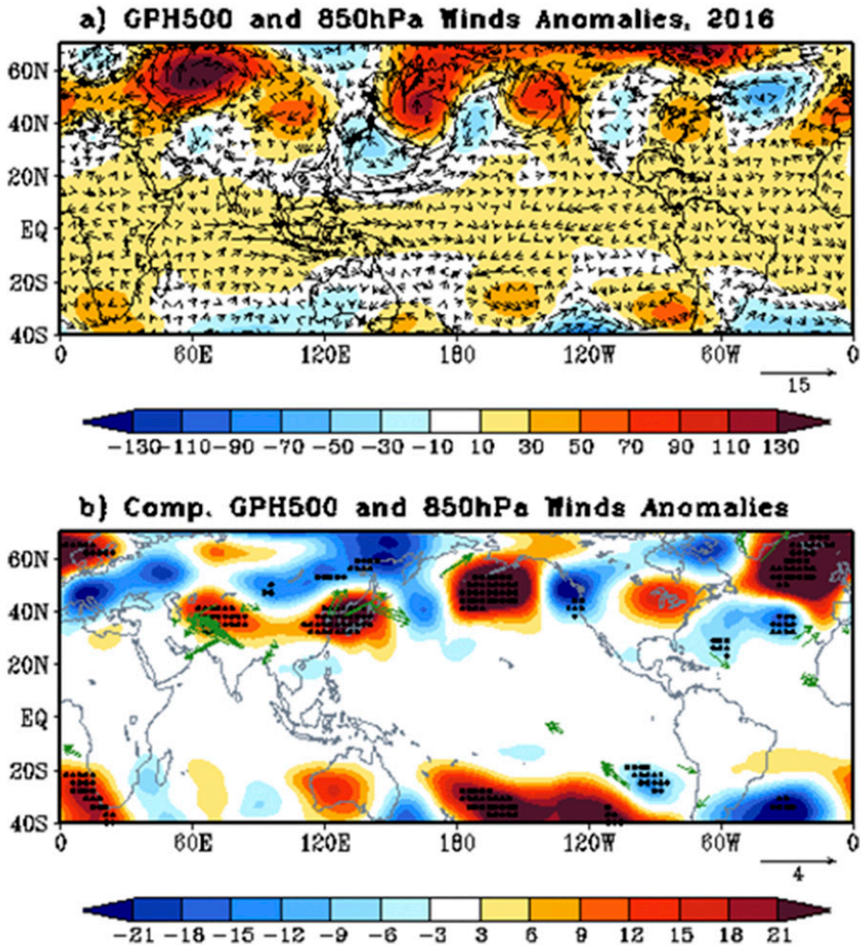

FIG. 3. (a) Anomalies of geopotential height at 500 hPa (shading; m) and winds at 850 hPa (vector; m s^{-1}) in August 2016 using the CFSR dataset. (b) Composite of anomalous geopotential height at 500 hPa (shading; m) and winds at 850 hPa (vector; m s^{-1}) in 8 years (1984, 1990, 1994, 1995, 2006, and 2010). Note that the years of 2012 and 2013 are not included in (b) because of the issue of v-wind data availability. Dots and wind vectors in (b) denote the statistical significance at the 95% confidence level.

addition, in early and mid-August 2016, the daily mean surface temperature in South Korea was 3°–4°C higher than the climatological (1981–2010) daily mean temperature (Fig. 1b). In particular, the surface temperature from 1 to 25 August 2016 was 28.0°C, which was the record-high surface temperature since 1979 (KMA 2016).

While typical heat waves are episodic and occur on shorter time scales, the heat wave that occurred in August 2016 was not. High surface temperatures were observed throughout South Korea, especially in the northwestern area, including Seoul (Fig. 1c). In August 2016, the large-scale atmospheric circulation at 500 hPa, along with low-level (850 hPa) winds (Figs. 2a, 3a), was quite different from the typical atmospheric circulation structure leading to heat waves in South Korea, in which a north–south dipole pattern between the South China Sea and northeast Asia is dominant, with an anomalous high geopotential height over the Korean Peninsula (Lee and Lee 2016; see also Figs. 2c, 3b). Recently, Lee and Lee (2016) investigated the interannual variation of heat wave frequency in South Korea for 1973–2014 and examined its connection with large-scale atmospheric circulations to reveal the typical features associated with the heat waves over South Korea. Lee and Lee (2016) found that the Pacific–Japan pattern, which is referred to as the atmospheric teleconnection influencing the extratropical circulation over East Asia from the tropical western Pacific in the boreal summer on both on interannual and intraseasonal time scales (Nitta 1986; Kosaka and Nakamura 2006), is clear during the heat waves over the Korean Peninsula. And they further argued that enhanced deep convection in

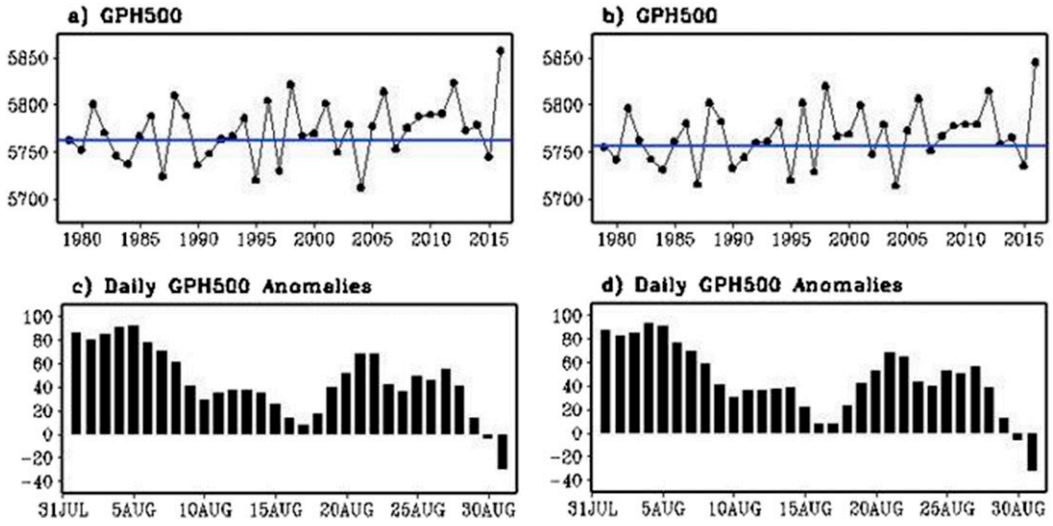

FIG. 4. Time series of 500-hPa geopotential height averaged on Kamchatka Peninsula (35°–55°N, 150°–175°E) in the (a) NCEP and (b) CFSR reanalysis datasets. A solid line indicates the climatological (1981–2010) mean. The daily geopotential height anomaly averaged in Mongolia (35°–50°N, 90°–120°E) in August 2016 in the (c) NCEP and (d) CFSR reanalysis datasets. The units for (a)–(d) are m.

the South China Sea acts as a source of Rossby wave trains along southerly wind that generates positive geopotential height anomalies around South Korea, leading to extreme hot and dry days in South Korea. Unlike previous typical heat wave events, the anomalous low geopotential height was located south of Japan, and the anomalous high geopotential height was observed in Mongolia and the Kamchatka Peninsula (Figs. 2a, 3a). This indicates that the mechanism leading to the August 2016 heat wave was quite different, compared to that of a typical heat wave in South Korea. The aim of the current study is to investigate the physical mechanisms that led to the high temperature in the August 2016 heat wave in South Korea to understand its specific atmospheric circulations, compared to previous ones. In particular, we pay attention to the role of convective forcing in the tropical Pacific affecting the anomalous atmospheric circulation around the Korean Peninsula through atmospheric teleconnections.

The rest of the paper is organized as follows. The data and method used in this study are outlined in section 2. In section 3, the overall features of Korean heat waves during August are displayed, and the mechanism associated with the August 2016 heat wave is examined. The final section discusses the results and presents a summary of this study.

2. Data and methods

Daily and monthly mean surface temperatures from 45 weather stations in South Korea for 1979–2016 were provided by the Korea Meteorological Administration. In addition, daily and monthly mean geopotential height, winds, surface temperature, and specific humidity were obtained from National Centers for Environmental Prediction–Department of Energy (NCEP–DOE) Reanalysis-2 datasets with 2.5° × 2.5° resolution for 1979–2016 (Kalnay et al. 1996). To test the robustness of the results, we also analyze the daily and monthly mean geopotential height, winds, and surface temperature datasets obtained from Climate Forecast System Reanalysis (CFSR) for 1979–2009 and Climate Forecast System, version 2, for 2010–16 with 0.5° × 0.5° resolution (Saha et al. 2010). Outgoing longwave radiation (OLR) was also obtained from NCEP. Monthly mean sea surface temperature (SST) was obtained from the Extended Reconstruction SST, version 4 (ERSST.v4) (Huang et al. 2015), with 2° × 2° resolution. Daily and monthly mean anomalies are defined as daily and monthly mean deviations from the climatological (1981–2010) mean. The statistical significance test used in this study is based on a Student's t test. The effective degrees of freedom used to calculate the statistical significance were obtained from Livezey and Chen (1983).

3. Results

To investigate the mechanism responsible for the high temperatures in the August 2016 heat wave, we first conduct a composite analysis to identify the typical structure of the atmospheric circulation and its associated convective forcing. Figure 2b displays the August

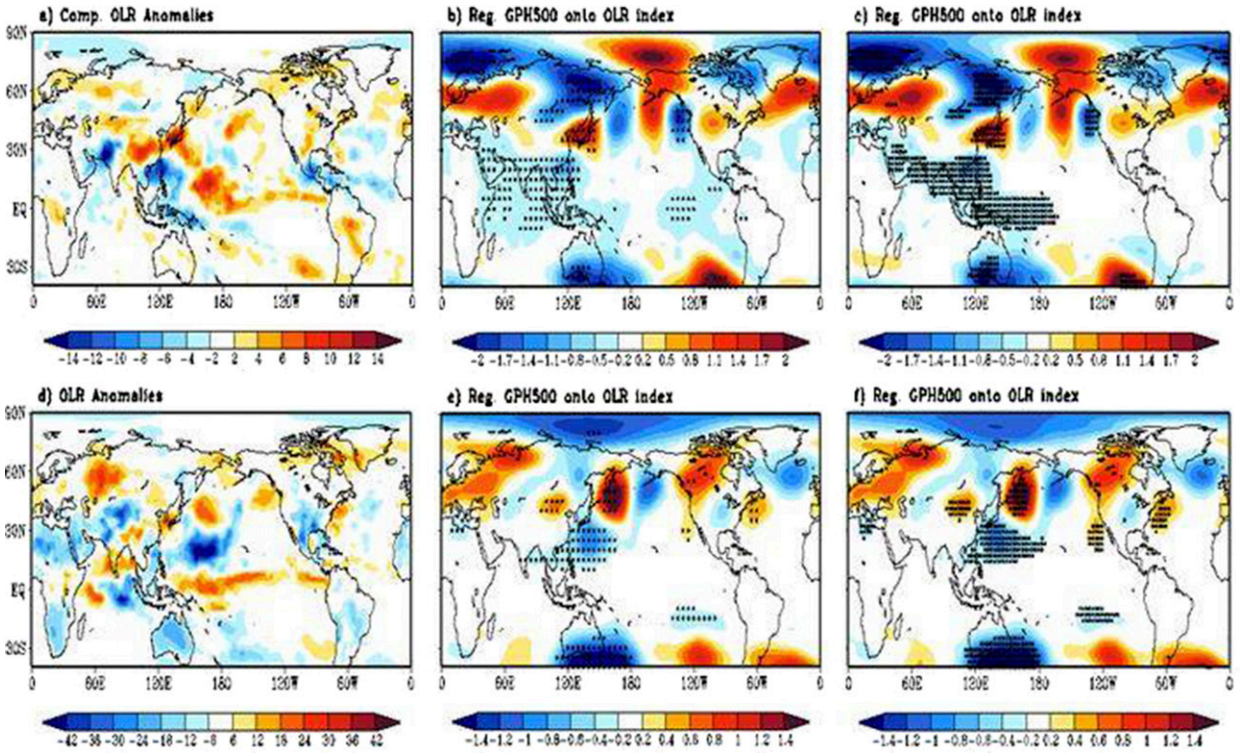

FIG. 5. (a) Composite of OLR anomaly in August in the HW_typ. Regressed geopotential height at 500 hPa from the (b) NCEP and (c) CFSR reanalysis datasets against the OLR averaged in the South China Sea and east of the Philippines (10°–25°N, 100°–140°E). (d) Spatial pattern of OLR anomalies in August 2016. (e),(f) As in (b),(c), but OLR is averaged in the western-to-central subtropical Pacific (15°–25°N, 150°E–180°). Units are (a),(d) W m^{-2} and (b),(c),(e),(f) m^3 W^{-1}. Note that we multiply by −1 in the regressed geopotential height map [(b),(c),(e),(f)] to represent the response of convective forcing. Dots in (b),(c),(e),(f) denote the statistical significance at the 90% confidence level.

surface temperature time series in South Korea for 1979–2016. We then select the years when the surface temperature is above one standard deviation (i.e., 1.19°C). Nine years (1984, 1990, 1994, 1995, 2006, 2010, 2012, 2013, and 2016) were selected, with a mean surface temperature of 26.6°C, which is much higher than the climatological temperature (25.1°C).

To compare with August 2016 (Fig. 2a), the composite analysis was based on 8 of the selected years (excluding 2016) to represent the large-scale atmospheric circulation of typical heat wave events in South Korea (hereafter, HW_typ). Figure 2c displays the composited geopotential height at 500 hPa with the low-level (850 hPa) wind. A wave train–like structure of atmospheric circulation, originating from the western tropical Pacific around the South China Sea and east of the Philippines, is dominant in the HW_typ. Note that a similar result is obtained when we select the years when the surface temperature is above 0.8 standard deviation (figure not shown). This is also found to some extent in August 2016, indicating that a convective forcing in the western tropical Pacific largely influences the atmospheric circulation, leading to August heat waves in South Korea. To test the robustness of atmospheric circulations associated with August 2016 and HW_typ, we also analyze the CFSR reanalysis dataset with a very high resolution of 0.5° × 0.5° (Figs. 3a,b). Similar results are obtained, compared with the NCEP reanalysis dataset (Figs. 2a,c). In August 2016, the anomalous low geopotential height was located south of Japan, and the anomalous high geopotential height was observed in Mongolia and the Kamchatka Peninsula (Fig. 3a). In the HW_typ, in contrast, the anomalous high geopotential height and its associated low-level southerly winds over the Korean Peninsula are dominant (Fig. 3b), which is statistically significant at the 95% confidence level. Note that we also analyze the observational features for 8 individual years in the HW_typ (figure not shown), and it is found that the anomalous high geopotential height is prominent around the Korean Peninsula in August for 8 individual years.

These composite analyses indicate that the mechanism leading to a typical August heat wave in the Korean Peninsula might be associated with two factors: radiative heating due to an increase of downward shortwave radiation and warm horizontal advection from the tropics, which are associated with the anomalous high geopotential height over the Korean Peninsula.

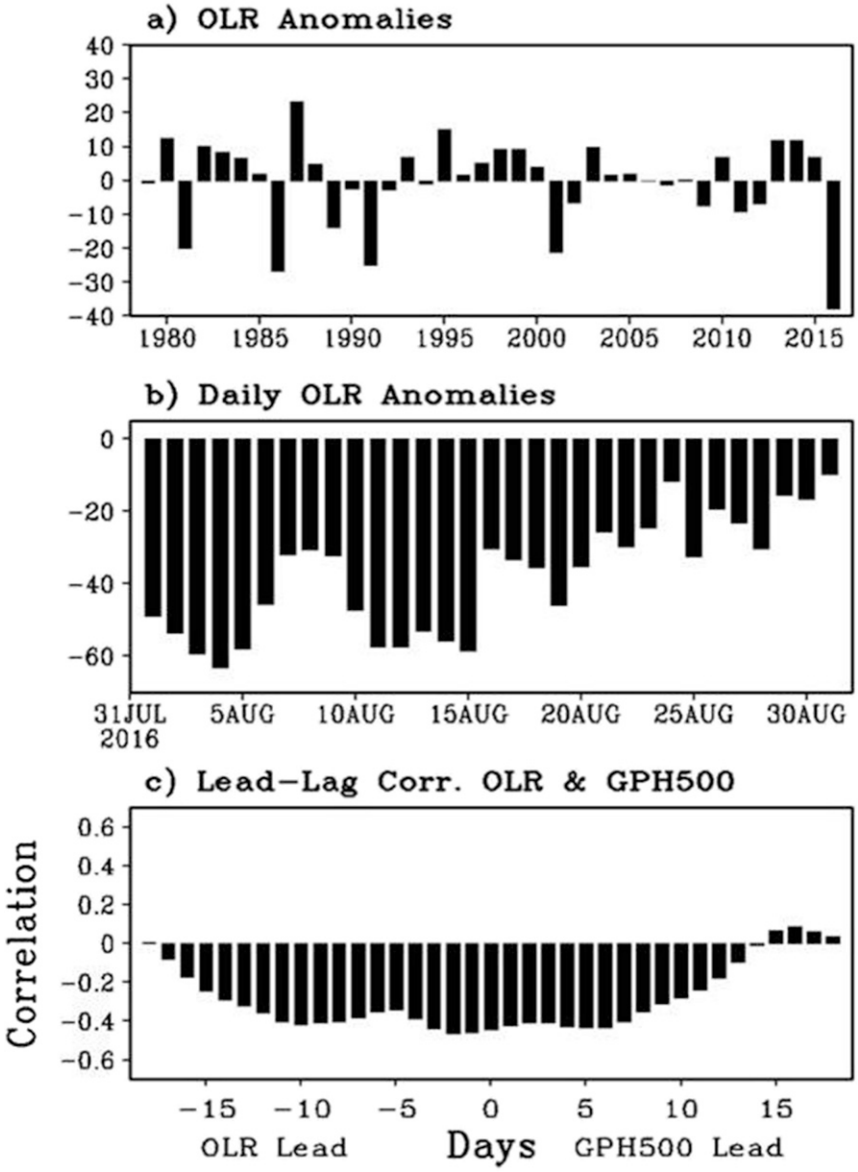

FIG. 6. (a) Time series of OLR anomalies (W m^{-2}) averaged in the western-to-central subtropical Pacific (15°–25°N, 150°E–180°) in August for 1979–2016. (b) Time series of daily OLR anomaly averaged in the western-to-central subtropical Pacific in August 2016. (c) Lead–lagged correlation between the daily OLR averaged in the western-to-central subtropical Pacific and the daily 500-hPa geopotential height averaged on the Kamchatka Peninsula for 1 Jul–30 Sep 2016.

In contrast, the anomalous low geopotential height and northeasterly winds at low level around the Korean Peninsula (Figs. 2a, 3a) indicate that the two aforementioned factors do not contribute significantly to the August 2016 heat wave. Another distinct feature of atmospheric circulation in August 2016, which was not observed in HW_typ, was the anomalous high geopotential height around Mongolia and the Kamchatka Peninsula. In particular, the intensity of the geopotential height over the Kamchatka Peninsula (35°–60°N, 145°E–180°) in August 2016 is the strongest since 1979 (Figs. 4a,b) in both the NCEP and CFSR reanalysis datasets. Furthermore, the time series of the daily geopotential height anomaly over the Kamchatka Peninsula (figure not shown) indicates that the anomalous geopotential height is persistently high in August 2016; therefore, it may act as an atmospheric blocking in the downstream region of the Korean Peninsula.

We argue that such a high geopotential height over the Kamchatka Peninsula acts to block the eastward

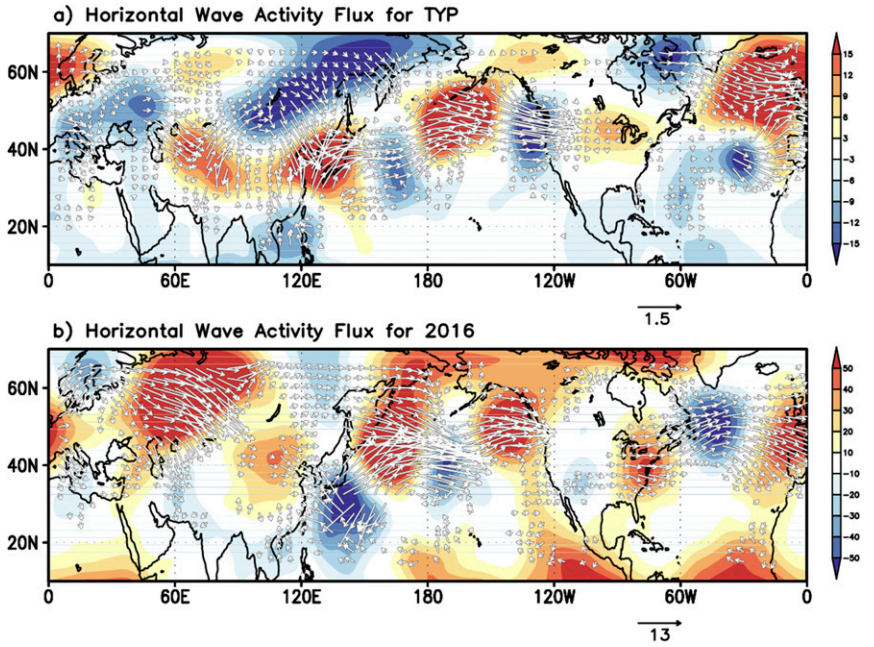

FIG. 7. Wave activity fluxes associated with a stationary Rossby wave train in (a) HW_typ and (b) August 2016. Contours are for 500-hPa monthly mean anomalous quasigeostrophic streamfunction, and arrows are for wave activity flux defined by Takaya and Nakamura (2001).

movement of the high geopotential height located in Mongolia, which was also persistent in August 2016 (Figs. 4c,d). Furthermore, very hot air conditions existed around not only Mongolia, but also the western Eurasian continent in August 2016 (Fig. 2d). Therefore, the anomalous high geopotential height over Mongolia (Fig. 2a) causes northerly winds with warm air into South Korea, contributing to the August 2016 heat wave. This result suggests that the anomalous high geopotential height over both Mongolia and the Kamchatka Peninsula played an important role in the South Korean heat wave. Hereafter, we pay attention to the mechanism that caused the anomalous low geopotential height below the Korean Peninsula, as well as high geopotential height over the Kamchatka Peninsula in August 2016.

To examine this, we first show the composite of OLR in HW_typ (Fig. 5a). A strong convection is observed in the South China Sea and east of the Philippines in the HW_typ (Fig. 5a), which is also consistent with the result in Lee and Lee (2016). They argued that the atmospheric circulation leading to heat waves in South Korea (Fig. 2c) was closely associated with enhanced convection in the South China Sea. Figures 5b and 5c display the regressed geopotential height at 500 hPa against the OLR averaged in the South China Sea and east of the Philippines (10°–25°N, 100°–140°E) using the NCEP and CFSR reanalysis datasets, respectively. By comparison, with the composite geopotential height at 500 hPa in HW_typ (Fig. 2c), it is evident that the anomalous high geopotential height over the Korean Peninsula is triggered by a strong convection in the South China Sea and east of the Philippines. Figures 5e and 5f are the same as in Figs. 5b and 5c, except in August 2016. In contrast to HW_typ, the center of the strong convection is clearly shifted to the east. Note that the intensity of OLR averaged in the western-to-central subtropical Pacific (15°–25°N, 150°E–180°) in August 2016 is the strongest since 1979 (Fig. 6a). Such an enhanced convective forcing in the western-to-central subtropical Pacific triggers a source for a Rossby wave train, which generates the anomalous low and high geopotential heights in the western tropical Pacific and the Kamchatka Peninsula, respectively (Figs. 5e,f). The Rossby wave train is located in the northwest region of enhanced convective forcing in the western-to-central subtropical Pacific (Figs. 5d–f). This represents a typical Matsuno–Gill-type response (Gill 1980; Matsuno 1966), which is characterized by the quasi-steady response via the Rossby waves to a given atmospheric heating in the tropics. A diabatic heating in the tropics could produce low-level westerly inflow in the northwest away from the heating region because of planetary wave propagation (Gill 1980). In addition, we calculate the pattern correlation coefficient between the 500-hPa geopotential anomaly in August 2016 (Fig. 2a) and the regressed 500-hPa geopotential against with the OLR anomalies

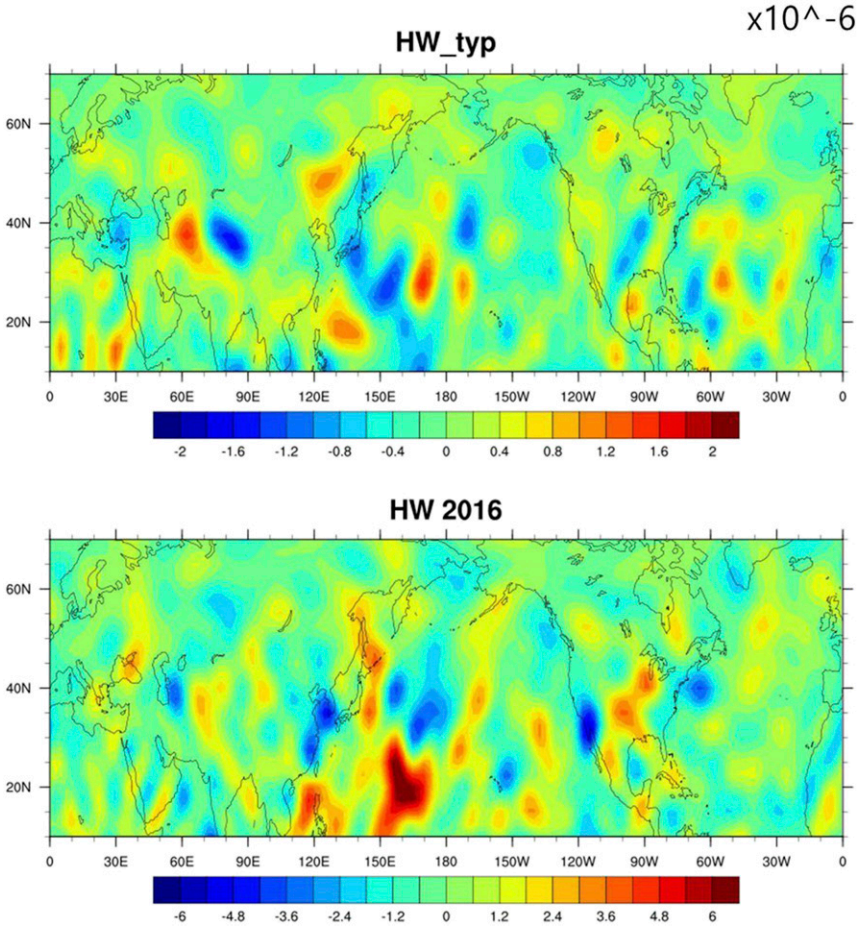

FIG. 8. Divergence fields (s^{-1}) at 200 hPa in (top) HW_typ and (bottom) August 2016.

averaged in the western-to-central subtropical Pacific (Fig. 5e) in the Northern Hemisphere, which is statistically significant at the 95% confidence level, 0.61.

Figure 6b displays the time series of daily OLR anomaly averaged in the western-to-central subtropical Pacific in August 2016, indicating that strong convective forcing existed persistently in August 2016. We also calculate the lead–lagged correlation between the daily OLR in the western-to-central subtropical Pacific and the daily geopotential height averaged over the Kamchatka Peninsula for 1 July–31 September 2016 (Fig. 6c). The maximum correlation coefficient is −0.38, which is statistically significant at the 95% confidence level, when the OLR leads the geopotential height at a 2-day lead time. This indicates that the convective forcing in the western-to-central subtropical Pacific directly induces the geopotential height over the Kamchatka Peninsula with daily scale lagged time. Therefore, we argue that the strong convection in the western-to-central subtropical Pacific plays a key role in the August 2016 heat wave by inducing the anomalous high geopotential height over the Kamchatka Peninsula through atmospheric teleconnections.

To further examine the Rossby wave train in HW_typ and August 2016, we calculate wave activity fluxes following Takaya and Nakamura (2001) (Fig. 7),

$$\mathbf{W} = \frac{p\cos\phi}{2|\mathbf{U}|}\left\{\begin{array}{l} \dfrac{U}{a^2\cos^2\phi}\left[\left(\dfrac{\partial\psi'}{\partial\lambda}\right)^2 - \psi'\dfrac{\partial^2\psi'}{\partial\lambda^2}\right] + \dfrac{V}{a^2\cos\phi}\left[\dfrac{\partial\psi'}{\partial\lambda}\dfrac{\partial\psi'}{\partial\phi} - \psi'\dfrac{\partial^2\psi'}{\partial\lambda\,\partial\phi}\right] \\ \quad + \dfrac{U}{a^2\cos\phi}\left[\dfrac{\partial\psi'}{\partial\lambda}\dfrac{\partial\psi'}{\partial\phi} - \psi'\dfrac{\partial^2\psi'}{\partial\lambda\,\partial\phi}\right] + \dfrac{V}{a^2}\left[\left(\dfrac{\partial\psi'}{\partial\phi}\right)^2 - \psi'\dfrac{\partial^2\psi'}{\partial\phi^2}\right] \end{array}\right\},$$

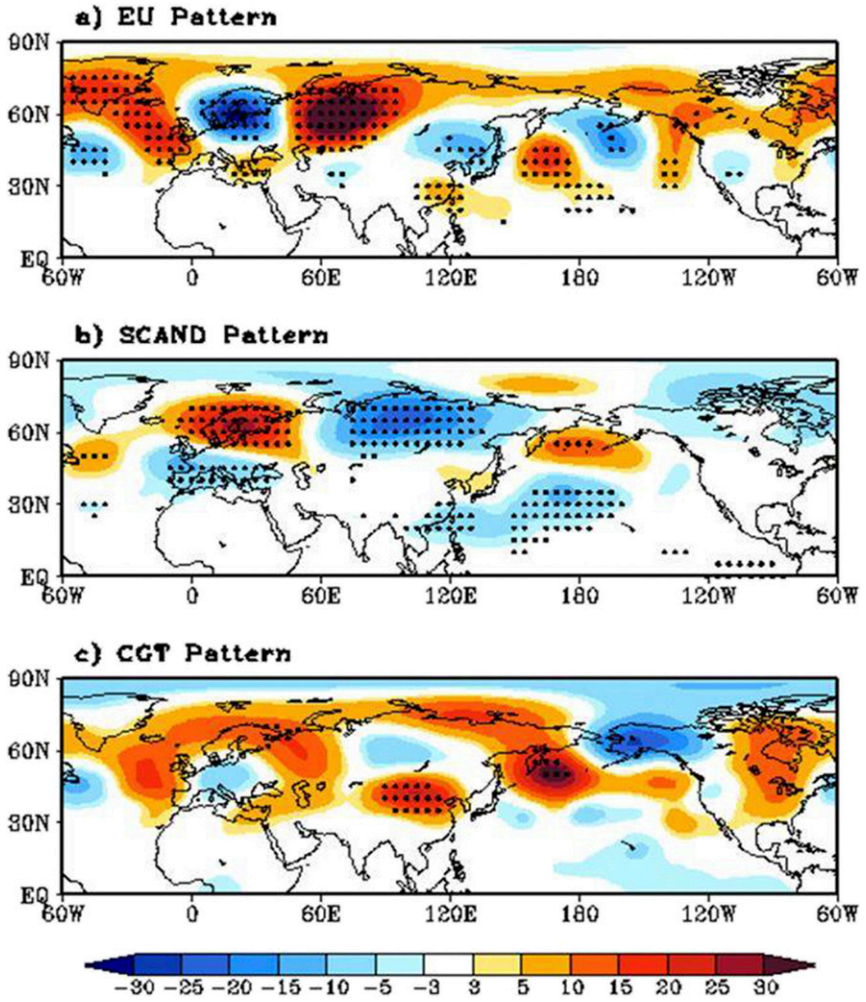

FIG. 9. Spatial pattern of regressed geopotential height with the (a) EU, (b) SCAND, and (c) CGT indexes for 1979–2016 during August. Dots denote the statistical significance at the 95% confidence level.

where **W** is wave-activity flux, p is normalized pressure, U and V are basic flow, λ is longitude, ϕ is latitude, a is Earth's radius, ψ' is streamfunction, f_0 is Coriolis parameter, and N^2 is buoyancy frequency.

While the vectors in Fig. 7 represent the direction of the stationary wave, the wave's magnitude indicates the group velocity of Rossby waves. It is evident that wave fluxes originate from the South China Sea, where the convective forcings are dominant in HW_typ (Fig. 7a). On the other hand, it is found that a stationary Rossby wave train, which originates from the western-to-central subtropical Pacific, propagates to the Korean Peninsula in August 2016. This result supports the notion that a wave train–like structure of atmospheric circulation that originated from the western tropical Pacific around the South China Sea is dominant in the HW_typ. In contrast, the Rossby wave train, which propagates onto the Korean Peninsula, originated from the western-to-central subtropical Pacific, where the strong convective forcings exist persistently in August 2016. To support this result, we also conduct the composite of divergence fields at 200 hPa in HW_typ and 2016 (Fig. 8). It is evident that the divergence at the upper level (200 hPa) is strong in the western-to-central subtropical Pacific, where a stationary Rossby wave train propagates to the Korean Peninsula in August 2016 (Fig. 8b). In contrast, an upper-level divergence in HW_typ is dominant around the South China Sea, which is associated with a wave train–like structure of atmospheric circulation onto the Korean Peninsula.

4. Discussion and summary

In this study, we explored the mechanism that led to the heat wave in South Korea in August 2016. It was

found that this heat wave was quite different from a typical heat wave in terms of its associated atmospheric circulation, as well as the structure of convective forcing in the tropical Pacific. Typical heat waves in South Korea during August result from a wave train–like structure of atmospheric circulation that originates around the South China Sea and cause an anomalous high geopotential height over the Korean Peninsula. However, we cannot exclude the possibility that other factors may contribute to the anomalously high geopotential height over the Korean Peninsula, in addition to the strong convection over the South China Sea. To briefly examine this, we calculate the regressed geopotential height with the Eurasian (EU) index (Wallace and Gutzler 1981), Scandinavian (SCAND) index (Barnston and Livezey 1987), and circumglobal teleconnection (CGT) index (Ding and Wang 2005) for 1979–2016 during August. Figure 9 indicates that the zonal wave train associated with the EU index is significantly associated with the geopotential height over the Korean Peninsula during August. However, the EU index has a negative sign in some years and a positive sign in other years in HW_typ (figure not shown). Therefore, the zonal wave train originated from the Eurasian continent may or may not contribute to the anomalous high geopotential height over the Korean Peninsula.

On the other hand, an anomalous high geopotential height over both the Kamchatka Peninsula and Mongolia played a key role in inducing the August 2016 heat wave. In addition, high geopotential height over the Kamchatka Peninsula may act to block the eastward movement of the high geopotential height over Mongolia, which advected warm air into South Korea. We further showed that the strongest convective forcing in the western-to-central subtropical Pacific directly induced a wavelike atmospheric circulation from the western tropical Pacific to the Kamchatka Peninsula. However, it should be noted that the CGT pattern, whose index is a positive sign in 2016, is significantly associated with the anomalous high geopotential height around Mongolia and the Kamchatka Peninsula (Fig. 9c), which may contribute to the heat wave in August 2016. Furthermore, we analyze the OLR anomalies, as well as 500-hPa geopotential height, for 4 years (1981, 1986, 1991, and 2001) when the convective forcing in the western-to-central subtropical Pacific during August was strong, like in August 2016 (figure not shown). While the Rossby wave train from the subtropics to the North Pacific, like 2016, was observed for 3 years (1981, 1986, and 2001), the intensity of anomalous high pressure around northern China and Mongolia was weak. On the other hand, the anomalous high geopotential height over the Kamchatka Peninsula was not observed in August 1991, in contrast to 2016. This result also indicates that both the anomalous high geopotential height in Mongolia and the anomalous high geopotential height over the Kamchatka Peninsula play a role to induce the heat wave in August 2016.

We do not explore why the strongest convective forcing occurred in the western-to-central subtropical Pacific in August 2016. Such a strong convective forcing might be associated with the La Niña–like cooling in August 2016; however, it is not clear yet. In addition, it is necessary to examine what caused the warm condition over Mongolia in August 2016, as well as the anomalous high geopotential height (Figs. 2a,d). This might be associated with land–atmosphere interactions that need to be addressed. Last, we acknowledge the main caveat in the present study: the sample size used to create the composite for the "typical years" is small; therefore, we cannot exclude the possibility that the typical atmospheric circulation structure leading to heat waves in South Korea could be induced by chance.

Acknowledgments. Daily and monthly mean surface temperatures from 45 weather stations in South Korea for 1979–2016 were provided by the Korea Meteorological Administration. Outgoing longwave radiation dataset can be found at http://www.esrl.noaa.gov/psd/map/clim/olr.html. Daily and monthly mean geopotential height, winds, and surface temperature can be obtained from National Centers for Environmental Prediction–Department of Energy (NCEP–DOE) Reanalysis-2 datasets (http://www.esrl.noaa.gov/psd/data/gridded/data.ncep.reanalysis.html). Daily and monthly geopotential height was provided by the Climate Forecast System Reanalysis (CFSR) (https://rda.ucar.edu/pub/cfsr.html). In addition, the monthly mean SST was from the Extended Reconstruction SST, version 4 (ERSST.v4) (https://www.ncdc.noaa.gov/data-access/marineocean-data/extended-reconstructed-sea-surface-temperature-ersst-v4). This work was supported by the Korea Meteorological Administration Research and Development Program under Grant KMIPA 2015–2112. SWY is also supported by the National Strategic Project-Fine particle of the National Research Foundation of Korea (NRF), funded by the Ministry of Science and ICT (MSIT), the Ministry of Environment (ME), and by the Ministry of Health and Welfare (MOHW) NRF-2017M3D8A1092022.

REFERENCES

Barnston, A., and R. E. Livezey, 1987: Classification, seasonality and persistence of low-frequency atmospheric circulation patterns. *Mon. Wea. Rev.*, **115**, 1083–1126, https://doi.org/10.1175/1520-0493(1987)115<1083:CSAPOL>2.0.CO;2.

Cerne, S. B., C. S. Vera, and B. Liebmann, 2007: The nature of a heat wave in eastern Argentina occurring during SALLJEX.

Mon. Wea. Rev., **135**, 1165–1174, https://doi.org/10.1175/MWR3306.1.

Coumou, D., and S. Rahmstorf, 2012: A decade of weather extremes. *Nat. Climate Change*, **2**, 491–496, https://doi.org/10.1038/nclimate1452.

——, and A. Robinson, 2013: Historic and future increase in the global land area affected by monthly heat extremes. *Environ. Res. Lett.*, **8**, 034018, https://doi.org/10.1088/1748-9326/8/3/034018.

——, V. Petoukhov, S. Rahmstorf, S. Petri, and H. J. Schellenhuber, 2014: Quasi-resonant circulation regimes and hemispheric synchronization of extreme weather in boreal summer. *Proc. Natl. Acad. Sci. USA*, **111**, 12 331–12 336, https://doi.org/10.1073/pnas.1412797111.

——, J. Lehmann, and J. Beckmann, 2015: The weakening summer circulation in the Northern Hemisphere mid-latitudes. *Science*, **348**, 324–327, https://doi.org/10.1126/science.1261768.

Di Capua, G., and D. Coumou, 2016: Changes in meandering of the Northern Hemisphere circulation. *Environ. Res. Lett.*, **11**, 094028, https://doi.org/10.1088/1748-9326/11/9/094028.

Ding, Q., and B. Wang, 2005: Circumglobal teleconnection in the Northern Hemisphere summer. *J. Climate*, **18**, 3483–3505, https://doi.org/10.1175/JCLI3473.1.

Galarneau, T. J., Jr., T. M. Hamill, R. M. Dole, and J. Perlwitz, 2012: A multiscale analysis of the extreme weather events over western Russia and northern Pakistan during July 2010. *Mon. Wea. Rev.*, **140**, 1639–1664, https://doi.org/10.1175/MWR-D-11-00191.1.

García-Herrera, G., J. Díaz, R. M. Trigo, J. Luterbacher, and E. M. Fischer, 2010: A review of the European summer heat wave of 2003. *Crit. Rev. Environ. Sci. Technol.*, **40**, 267–306, https://doi.org/10.1080/10643380802238137.

Gill, A. E., 1980: Some simple solutions for heat-induced tropical circulation. *Quart. J. Roy. Meteor. Soc.*, **106**, 447–462, https://doi.org/10.1002/qj.49710644905.

Grotjahn, R., and Coauthors, 2016: North American extreme temperature events and related large scale meteorological patterns: A review of statistical methods, dynamics, modeling, and trends. *Climate Dyn.*, **46**, 1151–1184, https://doi.org/10.1007/s00382-015-2638-6.

Huang, B., and Coauthors, 2015: Extended Reconstructed Sea Surface Temperature version 4 (ERSST.v4). Part I: Upgrades and intercomparisons. *J. Climate*, **28**, 911–930, https://doi.org/10.1175/JCLI-D-14-00006.1.

IPCC, 2013: *Climate Change 2013: The Physical Science Basis*. Cambridge University Press, 1535 pp., https://doi.org/10.1017/CBO9781107415324.

Jones, P., D. Lister, T. Osborn, C. Harpham, M. Salmon, and C. Morice, 2012: Hemispheric and large-scale land-surface air temperature variations: An extensive revision and an update to 2010. *J. Geophys. Res.*, **117**, D05127, https://doi.org/10.1029/2011JD017139.

Kalnay, E., and Coauthors, 1996: The NCEP/NCAR 40-Year Reanalysis Project. *Bull. Amer. Meteor. Soc.*, **77**, 437–472, https://doi.org/10.1175/1520-0477(1996)077<0437:TNYRP>2.0.CO;2.

Karl, T. R., and R. G. Quayle, 1981: The 1980 summer heat wave and drought in historical perspective. *Mon. Wea. Rev.*, **109**, 2055–2073, https://doi.org/10.1175/1520-0493(1981)109<2055:TSHWAD>2.0.CO;2.

Kim, C. G., S. M. Lee, H. K. Jeong, J. K. Jang, Y. H. Kim, and C. K. Lee, 2010: *Impacts of Climate Change on Korean Agriculture and Its Counterstrategies*. Korea Rural Economics Institute, 306 pp.

KMA, 2016: Weather characteristic in August 2016 (in Korean). Korea Meteorological Administration Rep., 17 pp., http://web.kma.go.kr/notify/press/kma_list.jsp?bid=press&mode=view&num=1193250&page=11&field=&text=.

Kosaka, Y., and H. Nakamura, 2006: Structure and dynamics of the summertime Pacific–Japan teleconnection pattern. *Quart. J. Roy. Meteor. Soc.*, **132**, 2009–2030, https://doi.org/10.1256/qj.05.204.

Kysely, J., and J. Y. Kim, 2009: Mortality during heat waves in South Korea, 1991 to 2005: How exceptional was the 1994 heat wave? *Climate Res.*, **38**, 105–116, https://doi.org/10.3354/cr00775.

Lee, W. K., H. A. Lee, Y. H. Lim, and H. Park, 2016: Added effect of heat wave on mortality in Seoul, Korea. *Int. J. Biometeor.*, **60**, 719–726, https://doi.org/10.1007/s00484-015-1067-x.

Lee, W. S., and M. I. Lee, 2016: Interannual variability of heat waves in South Korea and their connection with large-scale atmospheric circulation patterns. *Int. J. Climatol.*, **36**, 4815–4830, https://doi.org/10.1002/joc.4671.

Livezey, R. E., and W. Y. Chen, 1983: Statistical field significance and its determination by Monte Carlo techniques. *Mon. Wea. Rev.*, **111**, 46–59, https://doi.org/10.1175/1520-0493(1983)111<0046:SFSAID>2.0.CO;2.

Matsuno, T., 1966: Quasi-geostrophic motions in the equatorial area. *J. Meteor. Soc. Japan*, **44**, 25–43, https://doi.org/10.2151/jmsj1965.44.1_25.

Meehl, G. A. and C. Tebaldi, 2000: More intense, more frequent, and longer lasting heat waves in the 21st century. *Science*, **305**, 994–997, https://doi.org/10.1126/science.1098704.

Min, S. K., Y. H. Kim, M. K. Kim, and C. Park, 2014: Assessing human contribution to the summer 2013 Korean heat wave [in "Explaining Extreme Events of 2013 from a Climate Perspective"]. *Bull. Amer. Meteor. Soc.*, **95** (9), S48–S51.

Nitta, T., 1986: Long-term variations of cloud amount in the western Pacific region. *J. Meteor. Soc. Japan*, **64**, 373–390, https://doi.org/10.2151/jmsj1965.64.3_373.

Saha, and Coauthors, 2010: The NCEP Climate Forecast System Reanalysis. *Bull. Amer. Meteor. Soc.*, **91**, 1015–1058, https://doi.org/10.1175/2010BAMS3001.1.

Takaya, K., and H. Nakamura, 2001: A formulation of a phase independent wave-activity flux for stationary and migratory quasigeostrophic eddies on a zonally varying basic flow. *J. Atmos. Sci.*, **58**, 608–627, https://doi.org/10.1175/1520-0469(2001)058<0608:AFOAPI>2.0.CO;2.

Wallace, J. M., and D. S. Gutzler, 1981: Teleconnections in the geopotential height field during the Northern Hemisphere winter. *Mon. Wea. Rev.*, **109**, 784–812, https://doi.org/10.1175/1520-0493(1981)109<0784:TITGHF>2.0.CO;2.

WMO, 2013: *The Global Climate 2001–2010: A Decade of Climate Extremes.* World Meteorological Organization, 110 pp.

Yeo, S.-R., S.-W. Yeh, Y. Won, H.-S. Jo, and W. Kim, 2017: Distinct mechanisms of Korean surface temperature variability during early and late summer. *J. Geophys. Res. Atmos.*, **122**, 6137–6151, https://doi.org/10.1002/2017JD026458.

——, ——, Y. Kim, and S.-Y. Yim, 2018: Monthly climate variation over Korea in relation to the two types of ENSO evolution. *Int. J. Climatol.*, **38**, 811–824, https://doi.org/10.1002/joc.5212.